

Analysis of Functional Brain Images Using Population-Based Probabilistic Atlas

Jae Sung Lee and Dong Soo Lee*

Department of Nuclear Medicine, Seoul National University College of Medicine, Seoul, Korea

Abstract: Advances in imaging technology in the past decades have allowed profound insights into the human brain function and anatomy for normal and pathological conditions. Population-based probabilistic atlases (probabilistic map) for structural and functional anatomy of the brain have been developed using MRI, SPECT, and cytoarchitectonic data and provide a standard framework for functional brain data analysis. For example, automated delineation of the volume of interest (VOI) using the probabilistic maps of individual brain structures predefined on standard templates provides an efficient way for the objective assessment of image intensity and the underlying physiologies reflected by that image intensity. This review will focus on the development of the population-based atlases and application studies proving the utility of the atlases in basic neuroscience and the clinical assessment of brain disorders.

Key words: Brain, atlas, probabilistic map, quantification, functional brain mapping.

INTRODUCTION

Population-based probabilistic brain atlas (or probabilistic map) provides the information about the structural and functional anatomy of any given position in the stereotaxic standard space (Fig. 1). The probabilistic maps are useful in analyzing the structure and function of the brain that is complex and individually variable [1,2]. The location of the activated foci in the functional brain mapping studies could be labeled easily and reproducibly using the probabilistic maps [3-5]. The probabilistic maps could also be utilized as the standardized volume of interest (VOI) (or region of interest, ROI) to estimate the regional intensity of the brain image data [6] (Fig. 2).

Conventionally, the VOI has been manually drawn by the image specialist with the prior knowledge on structural and/or functional brain anatomy. However, the boundary of the manually drawn VOI is inevitably dependent on the operator and lacks the reproducibility [7,8]. Drawing VOI is also very laborious and time-consuming procedure especially if it has to be drawn across the multiple slices to reduce the statistical fluctuation in mean intensity within the VOI. Discontinuity in the boundary shown in other orthogonal direction is another drawback. To overcome these problems, delineation of the VOI definition in 3D space has to be automated with high accuracy and reproducibility [6-8]. Fortunately, there have been remarkable advances in spatial normalization techniques by which the anatomical differences between individual 3D brain images can be removed [9-11]. Individual images are warped to match their homologous spatial features to those of single target brain (or standard template). If the spatial normalization of a given image is successful, the VOI predefined on standard templates could be applied to the

warped image to calculate the mean intensity within the VOI. The reverse procedure (transformation of the predefined VOI onto the individual images) is also possible by inverting the spatial transformation using the deformation fields and global transformation parameters obtained during the spatial normalization. With the refined methods of spatial normalization, functional brain images could be analyzed objectively without operator bias and based on the population characteristics of anatomical and even functional (cytoarchitectonic) shapes.

This review will focus on the development of the population-based atlases based on anatomical and cytoarchitectonic features and successful application studies proving the utility of these atlases in basic neuroscience and the clinical assessment of brain disorders.

PROBABILISTIC ATLASES

MRI-Based Anatomical Map

Talairach and Tournoux's brain atlas is the most commonly used coordinate space for brain mapping studies [12]. Detailed anatomical description including Brodmann areas (BA) provided in this atlas is referred when researchers report the location of brain areas in the stereotaxic space. An automated system to retrieve brain labels from this atlas, called Talairach Daemon, was also developed to facilitate the consistent and comprehensive labeling of functional activation foci [3]. The Talairach atlas, however, does not properly represent the in-vivo anatomy of subjects since it is based on post mortem sections of a 60-year-old female subject. The variable slice separations, from 3 to 4 mm, and inconsistency in the data from the orthogonal planes are other limitations of the Talairach atlas to be used as a standard template for brain mapping studies [2, 13].

To overcome these limitations of the Talairach atlas, templates based on MRI data that have the intrinsic three-dimensional spatial coordinates have been developed. MRI data set collected over 300 young normal controls were transformed into stereotaxic space and averaged to generate

*Address correspondence to this author at the Department of Nuclear Medicine, Seoul National University College of Medicine, 28 Yungun-Dong, Chongno-Ku, Seoul 110-799, Korea; Tel: 82-2-760-2501; Fax: 82-2-745-7690; E-mail: dsl@palza.snu.ac.kr

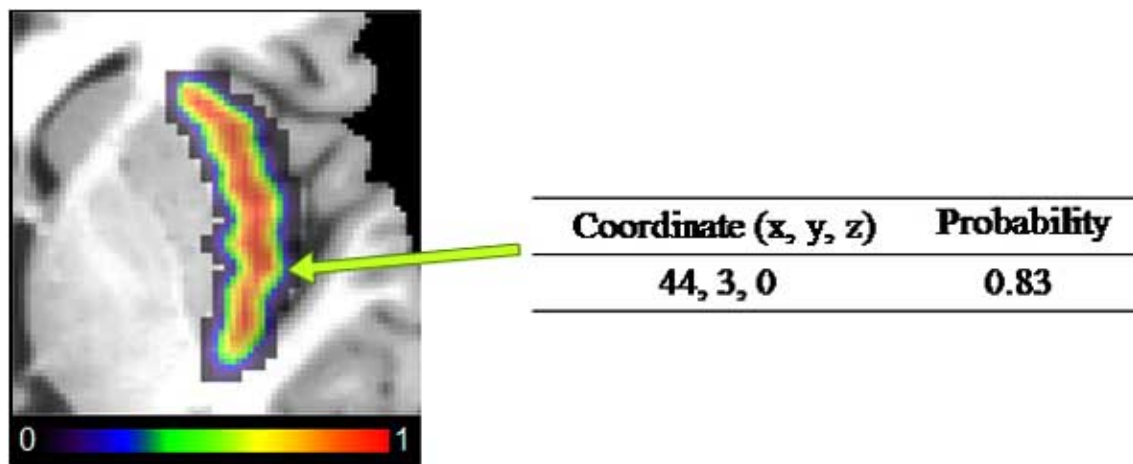


Fig. (1). Probabilistic map of the right insular cortex superimposed on T1 MRI Template.

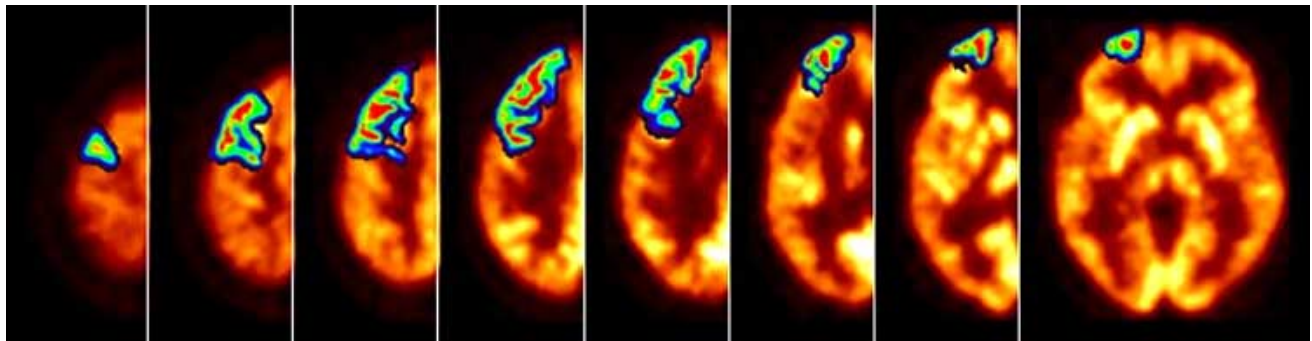


Fig. (2). Probabilistic volumes of interest: regional intensity in the brain images can be quantified by averaging regional intensities which were weighted using the probabilistic maps.

an MRI-based standard anatomical atlas by the Montreal Neurological Institute (MNI) [14,15]. MNI template based on 305 subjects is the official standard for the ICBM (International Consortium for Brain Mapping) stereotaxic space, and most widely used for human brain mapping studies as they were adopted by the Statistical Parametric Mapping (SPM, Institute of Neurology, University College of London, UK) program [16]. However, the MNI templates do not completely match to the Talairach atlas: the former is slightly larger than the latter. Because of this mismatch between the Talairach and MNI coordinates, the results of functional imaging studies based on MNI template can be misinterpreted if the Talairach atlas is referred to [7,13]. Although some algorithms to convert MNI coordinates to Talairach coordinates were proposed, errors in anatomical labelling are still present [13]. Use of the manually drawn 90 volumes of interest (VOI) on the MNI MRI single-subject brain were proposed for the automated and more accurate anatomical labelling in MNI coordinates [7]. However, the inter-individual variability in the local anatomy and intra- and inter-observer inconsistencies in anatomical parcellation are the inevitable drawbacks of this approach [8].

Population-based statistical data on anatomic labels at given positions account for the morphological variability in brain anatomy in population. MNI group constructed the

probabilistic maps of the anatomic labels based on MNI coordinates, and named this population-based atlas as SPAM (statistical probabilistic anatomy map) [17]. A probabilistic map was composed for each segmented structure in the stereotaxic space, by determining the proportion of subjects assigned a given anatomic label at each voxel position among the entire population. Anatomic labels on a stereotaxic target brain were transformed into the individual brain by the 3D nonlinear deformation for the automatic and consistent labelling, and subsequent linear transformation of the individual labels into the standard stereotaxic space were performed to create probabilistic maps called SPAM. Thus, the MNI SPAM consisted of macroscopic brain structures including multiple cortical gyri, white matter and cerebrospinal fluid space.

Although there have been remarkable advances in spatial normalization techniques for the brain as is explained in Introduction [9-11], the differences in the shape of the hemispheres and the sulcal pattern of brains relative to age, gender, races, and diseases could not be fully overcome by the available nonlinear spatial normalization techniques [2]. This necessity to account for those limitations in use of the templates and SPAM based on different ethnic groups motivated once the development of the age, gender and ethnic specific anatomical and functional brain templates

and MRI SPAM based on data of Korean healthy normal volunteers [8,18,19]. Probabilistic maps for 89 anatomical volumes of interest were developed utilizing the T-1 weighted SPGR (spoiled gradient echo) MRI data set of 75 normal volunteers, adopting the same procedures as was used for MNI SPAM [19] (Fig. 3).

MNI SPAM or in-house prepared probabilistic map can be used for the quantification of functional brain images. The anatomy-less functional images such as positron emission tomography (PET) or single photon emission computed tomography (SPECT) can now be quantified using the population-based anatomical information of SPAM. Though the PET or SPECT data are accompanied with the patients' own MRI data, SPAM-based quantification might be superior to patients' own MRI based one considering the efforts for correct registration of MRI and PET/ SPECT and the formidable shortcomings of individual manual drawing which would have been avoided if we used the population-based probabilistic approach.

Cytoarchitectonic Map

Anatomical units work sometimes as functional units but do not in other times. Almost hundred years ago, Brodmann did a marvelous and laborious job to parcellate the whole brain into functional units based on their cytoarchitectonic characteristics. Cytoarchitectonic means the cellular density, grouping, distribution and three-dimensional array. Cytoarchitectonic features can only be delineated on biopsied or autopsied specimen [20]. Although these

Brodman areas, the classic functional maps of the human cerebral cortex, should be used for interpreting the results of functional human brain data analysis, it is difficult to use the areas for exact scientific purposes because of the insufficient specification of the brain regions and vague boundaries between them [21]. Population-based cytoarchitectonic maps of human brain overcame these drawbacks. Once developed, population-based probabilistic maps based on cytoarchitectonic features and the quantification using these maps were readily accepted by the neuroimaging neuroscience community. Since cytoarchitectonics could not be identified in vivo, these probabilistic maps were constructed using autopsy brains which can be stained for their neuronal cell bodies, myelin and receptor architectures [20]. Neuronal cell bodies yielded a pattern of gray level intensity and this pattern became a clue to define the cytoarchitectonic border of adjacent areas. Subsequently, myelin and receptor distribution was also used to parcellate Brodmann areas [22]. Recently, receptor architectures in vivo and in vitro matched each other very well and so in the near future PET imaging receptors might be used to yield population-based cytoarchitectonic maps using in vivo data. The presently available functional cytoarchitectonic map, however, is the one derived from postmortem in vitro microscopic imaging data.

Cytoarchitectonic probabilistic maps of various brain areas including auditory, visual and motor cortices and Broca's areas were constructed and transformed onto the MRI template and are now available on the web page of Institut fuer Medizin (Forschungszentrum Juelich, Germany)

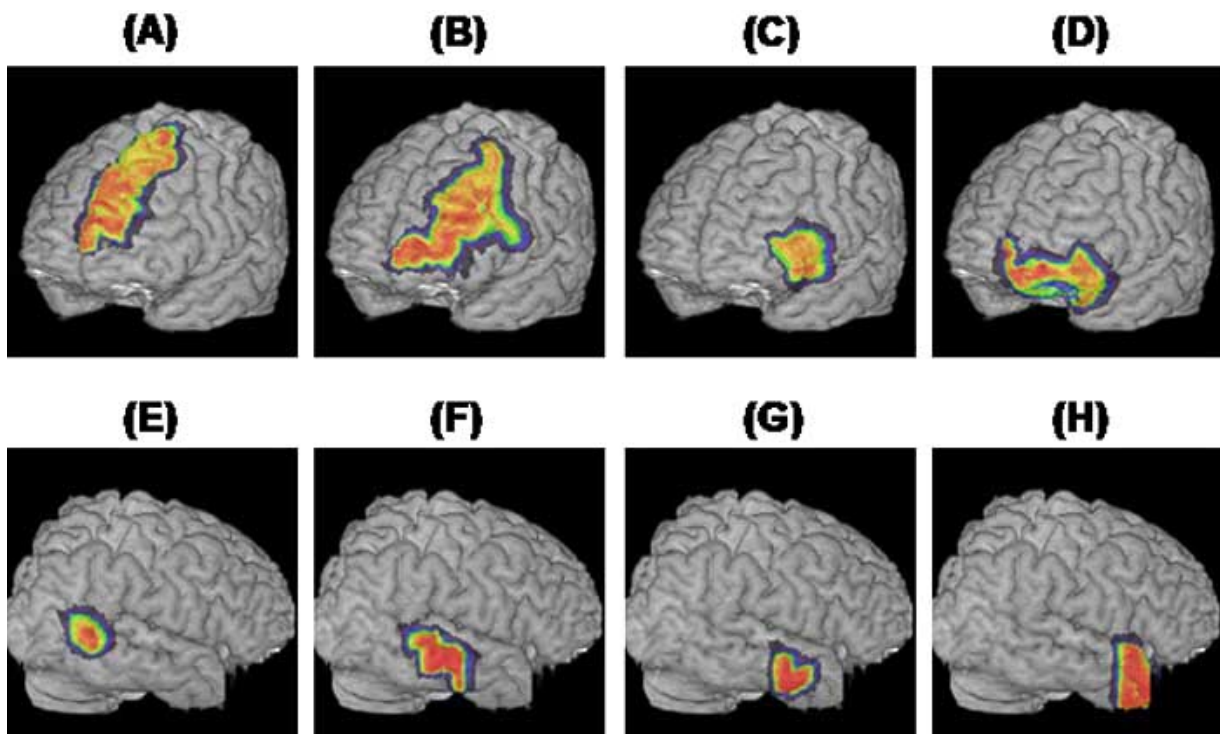


Fig. (3). Structural statistical probabilistic map based on MRI of Korean normal volunteers. (A) Superior frontal gyrus. (B) Middle frontal gyrus. (C) Inferior frontal gyrus. (D) Orbitofrontal gyrus. (E) Middle temporal gyrus, caudal part. (F) Middle temporal gyrus, intermediate part. (G) Middle temporal gyrus, rostral part. (H) Temporal pole.

[23]. In their long-lasting diligent work, post-mortem brains were obtained and scanned in an MR-scanner. These 3D MR images were used for correcting the shrinkage and distortions. After MRI scanning, all brains were dehydrated in graded alcohols, embedded in paraffin and serially sectioned. Images of the paraffin fixed brain were obtained after every 60th section with a CCD (charge-coupled device) digital camera. Every 60th histological section was stained for cell bodies, which yielded high contrast for cytoarchitectonic analysis. The volume of each brain was reconstructed from the paraffin-fixed brain images. Each reconstructed histological volume was spatially normalized to the reference brain using elastic transformation with full-multigrid. A number of cytoarchitectonic images were intensity-normalized and averaged on a voxel-by-voxel basis, at last producing one cytoarchitectonic map of a human brain. Unlike MRI-based probabilistic atlas, these cytoarchitectonic maps from only ten or dozen of humans were pooled to make a probabilistic atlas based on cytoarchitectonic features. Initial microscopic precision was rather blurred to yield visually-interpretable images of probabilistic maps on top of MRI template and thus we are now able to use these maps as templates of Brodman Areas 41, 44, 45, 17 and 18 etc [23].

Probabilistic Map of Vascular Territory

Population-based probabilistic map of the cerebrovascular system are another important tool for medical and scientific purposes. Although contrast angiography provides anatomical information about stenosis or new vessel formation after bypass surgery, it cannot directly provide information about tissue perfusion [24,25]. Functional images representing cerebral perfusion, such as the perfusion weighted or diffusion weighted MRI, perfusion SPECT and PET can be employed to construct the probabilistic maps for the vascular territory [26]. Brain SPECT images acquired after injection of Tc-99m-HMPAO into the internal carotid artery (ICA) during the intracarotid amobarbital procedure in epilepsy patients (IAP SPECT) provided superior anatomical information on the blood flow distribution from the ICA. This procedure used to be performed preoperatively to predict postoperative memory and language deficit after unilateral temporal lobectomy, and yielded very fine data regarding internal carotid arterial supply in population [27,28]. IAP SPECT during Wada test in epilepsy patients enabled the development of probabilistic maps of the distribution of blood supply from the ICA while SPECT images were transformed into the MNI stereotaxic coordinate [26] (Fig. 4). Basal brain SPECT images of the same individuals were spatially normalized into standardized SPECT template and the normalization parameters were reapplied to IAP SPECT images so that it could overcome the limitation of IAP SPECT images where radiotracer reached and so visualized limited brain areas.

Interestingly in vascular territory map, two kinds of probabilistic maps were made. Probabilistic map was constructed from individual binary contours of ICA territories, and in this case, the map looked the same as MRI-based anatomical maps. Each voxel on ICA SPECT map belonged to the ICA territory in probabilistic terms (0 to

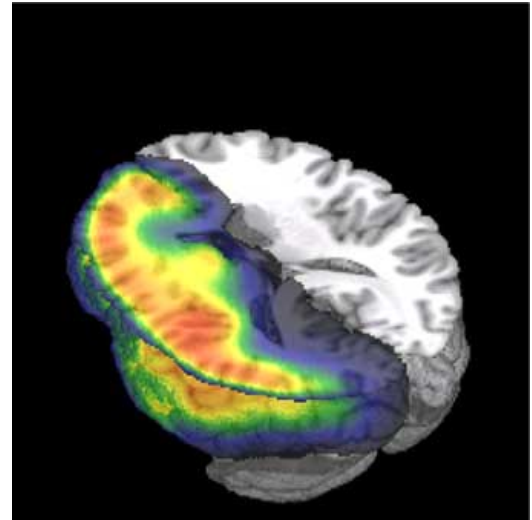


Fig. (4). Perfusion probabilistic maps of blood supply from the left ICA, superimposed on the surface of a SPM T1 MRI template.

100% among the population). The second one was the probabilistic map of vascular contribution from ICA and represented the fractional supply from ICA according to the tissue demand as well as the territorial variability. If other vascular contribution was significant as in inferior temporal areas (from posterior circulation), the probabilistic map represented both the individual variations of contour and the vascular contribution from ICA among population.

APPLICATIONS OF PROBABILISTIC ATLAS

Probabilistic Anatomical Labeling

MNI SPAM was used for new statistical techniques that integrate the anatomic variability in the assessment of functional imaging data by constraining the search space for significant activations in PET and SPECT imaging studies [29,30]. Dinov *et al.* used the SPAM to account for the morphological and spatial registration differences between two different functional data sets in the subvolume thresholding technique in which the threshold values for different regions of the brain were determined depending on their size and geometry [29].

Anatomical information provided by the probabilistic maps is useful for consistent and automatic labelling of the activation foci detected by the functional imaging studies. Retrieval of the anatomical information in Talairach space for a given point can be achieved by the Talairach Daemon [3]. Easy internet access to a 3D database of brain labels (MNI SPAM and Talairach atlas labels) is possible. When automatic labels by the Talairach Daemon and manual atlas-derived labels from an expert group were compared with the labels of activation foci from over 250 published studies, Talairach Daemon's match with author's labels was better than that of the expert group.

Program for searching the names of anatomical structures with non-zero probability and the probabilities that the given position belonged to the structures in the MNI coordinates were also developed [4,5]. Direct probabilistic labeling of activation foci in MNI coordinates would be easier and more accurate than the conversion of coordinates from the MNI to Talairach and subsequent referring the Talairach Daemon in the brain data analysis performed in MNI space.

Probabilistic Volume of Interest

Regional intensity in the brain images can be quantified by averaging regional intensities that were weighted using the probabilistic maps after normalization of the images spatially into the standard stereotaxic space where the probabilistic maps were constructed. MNI SPAM was first applied to obtain the normal range and the distribution of glucose uptake on F-18 fluorodeoxyglucose (FDG) PET [6]. Normal ranges for the asymmetric indices of six gyri of temporal lobes were established and used successfully to find out gyri of abnormal FDG uptake beyond a few standard deviations in normal population. Following this report, several investigations followed and also proved the utility of this approach [31-34].

In epilepsy studies, based on population-based analysis of F-18 FDG and O-15 water PET, uncoupling of metabolism and perfusion in the epileptogenic zones were found objectively [31], occipital lobe epilepsy was diagnosed [32], differential metabolic patterns of lateral and medial temporal lobe epilepsy were disclosed [33]. In a large cohort study of medial temporal lobe epilepsy, the extent and severity of hypometabolism of medial and lateral parts of temporal lobes were compared and no correlation with prognosis after surgery was definitively found [34]. Before this study, post-surgical prognostic implication of extent and severity of hypometabolism was contradictory in the literature [35,36]. In this study [34], the extent of the hypometabolic area in VOIs of frontal, temporal, parieto-occipital, and thalamic areas was determined by counting the number of voxels with significantly decreased hypometabolism in each VOI segmented by SPAM. Voxels with probability above 0.5 were included in each VOI and hypometabolic area was determined by the SPM analysis in which the individual patient's F-18-FDG brain PET image was compared with those of normal controls using T-statistics for each voxel.

Effects of the normal aging and gender difference on the regional heterogeneity of cerebral glucose metabolism in a large number of subjects was also investigated by employing the standardized VOI defined using the anatomical probabilistic information [37]. In this study, MNI SPAM were classified into whole gray matter, frontal lobe, parietal lobe, temporal lobe, occipital lobe, striatum, cingulate gyrus, brain stem, and cerebellum, and summed to compose the probabilistic maps for these 9 regions. Voxels with a probability above 0.5 were finally included in each VOI, and fractal dimensions, the quantitative measurement for the heterogeneity of cerebral glucose metabolism were calculated for these 9 brain regions.

Recently, the MRI SPAM based on neuroimaging data of Korean volunteers was used to explore the regionally

specific effects of aging on glucose metabolism in the cingulate cortex [8]. F-18-FDG PET images of 49 normal volunteers were spatially normalized onto the Korean PET template and the regional counts within the cingulate cortex were obtained using the probabilistic maps of rostral and caudal parts of anterior cingulate and posterior cingulate provided by the Korean SPAM database. This study showed that the glucose metabolism change in cingulate gyrus was regionally specific; ratios of glucose metabolism in rostral anterior cingulate versus posterior cingulate and caudal anterior cingulate versus posterior cingulate were significantly decreased as the age increased. 'Rostral anterior'/ 'posterior' was decreased by 3.1% per decade of age and 'caudal anterior'/ 'posterior' was decreased by 1.7%.

Brain PET and SPECT images have the spatial resolution of 4-6 mm and 8-12 mm which is in the same order as the thickness of gray matter in cortical surface and the size of the subcortical regions. Activity in the gray matter is therefore underestimated due to partial volume effect. Structural imaging studies have also shown age and disease-related loss of brain tissue degree of which is regionally specific as well. Therefore, the partial volume effect, due to cortical atrophy, would confound the results of investigation on the regional abnormality shown in the brain PET and SPECT images. This partial volume effect in PET or SPECT can be corrected by referring to the subject's own high-resolution MRI [38,39], and the quantification on partial volume-corrected images is possible by the spatial normalization of the images and application of the probabilistic VOI [40,41]. SPAM analysis showed that the age-related decline of regional glucose metabolism in frontal lobe was still significant after the MRI-based partial volume correction of the F-18-FDG PET [41].

The voxel-based image analysis such as the SPM (statistical parametric mapping) technique is now quite popular these days. After a decade of finding multiple activated foci of increased perfusion on water PET or functional MRI, people became interested in how activated brain areas played together. This new field of promising novel findings is called the search for functional connectivity. Post-hoc delineation of areas of interests is to be done in these brain activation studies, however, is also up to very much arbitrariness or bias. Regional counts of the probabilistic VOI can be used as a covariate to identify the brain regions that have the functional connectivity with the area defined by the probabilistic VOI. VOI's based on anatomical or cytoarchitectonic probabilistic maps have credit in two aspects. They are pre-defined and independently chosen from population-based data. Statistical dilemma can be prevented by a priori choice of VOI and if brain works on functional probabilistic map units, the analysis would include enough brain areas for further analysis of functional connectivity.

Altered functional connectivity of the auditory cortex in deaf subjects due to the loss of auditory input was investigated using 'the regional F-18-FDG PET count in the primary auditory cortex (BA41)' defined by the cytoarchitectonic probabilistic maps as the covariate in the interregional and interhemispheric correlation analysis [42]. The authors called this type of analysis as the interregional

correlation analysis. The cytoarchitectonic maps of the primary auditory cortex were also used to study the age-associated changes of cerebral glucose metabolic activity in the deaf children [43]. Of course, this method of defining VOI a priori can be used for brain activation water PET studies and routine functional MRI studies.

The quantification of regional cerebral perfusion in the ICA territory is especially important since the ICA is the vessel most frequently involved in major cerebrovascular diseases while it supplies blood to substantial parts of the brain [44,45]. Probabilistic maps of the distribution of blood supply from the ICA were used to assess the efficacy of the cerebral arterial bypass surgery in the patients with the ischemia in the ICA territory [46]. Basal and acetazolamide-stress brain SPECT of the patients obtained before and after the operation were compared with those of healthy normal controls by the SPM analysis (voxel-wise t-test). Subsequently, the extent of the ischemia (the number of voxels that showed significant hypoperfusion in SPM analysis) and regional counts within the ICA territory determined by the ICA probabilistic map were calculated, showing the improvement in cerebral perfusion and perfusion reserve after the bypass surgery.

CONCLUSIONS

Population-based probabilistic maps enable the consistent anatomical labeling of the brain regions in stereotaxic space and operator-independent delineation of VOI for the analysis of functional brain images. Structural, cytoarchitectonic and cerebrovascular probabilistic maps with information on anatomic and functional variability in a population were useful for finding out the abnormal or activated brain regions. Combination of voxel-based analysis and VOI analysis based on probabilistic maps would be the promising approach in the interpretation of brain data.

ACKNOWLEDGEMENTS

This work was supported in part by Brain Research Center of the 21st Century Frontier Research Program and in part by BK21 Human Life Sciences.

REFERENCES

- [1] Mazziotta J, Toga A, Evans A, *et al.* A probabilistic atlas and reference system for the human brain: International Consortium for Brain Mapping (ICBM). *Philos Trans R Soc Lond B Biol Sci* 2001; 356: 1293-322.
- [2] Toga AW, Thompson PM. *Maps of the brain*. *Anat Rec* 2001; 265: 37-53.
- [3] Lancaster JL, Woldorff MG, Parsons LM, *et al.* Automated Talairach atlas labels for functional brain mapping. *Hum Brain Mapp* 2000; 10: 120-31.
- [4] Kim JS, Lee DS, Lee BI, *et al.* Probabilistic anatomical labeling of brain structures using statistical probabilistic anatomical maps. *Korean J Nucl Med* 2002; 36: 317-24.
- [5] Lee JS, Wong DF, Zhou Y, Hoehn-Saric R. Localization of neural substrates of worry using H₂¹⁵O PET and probabilistic brain atlas. *J Cereb Blood Flow Metab* 2003; 23(S1): 713 [Abstract].
- [6] Kang KW, Lee DS, Cho JH, *et al.* Quantification of F-18 FDG PET images in temporal lobe epilepsy patients using probabilistic brain atlas. *Neuroimage* 2001; 14: 1-6.
- [7] Tzourio-Mazoyer N, Landeau B, Papathanassiou D, *et al.* Automated anatomical labeling of activations in SPM using a macroscopic anatomical parcellation of the MNI MRI single-subject brain. *Neuroimage* 2002; 15: 273-89.
- [8] Lee JS, Lee DS, Kim YK, *et al.* Quantification of brain images using Korean standard templates and structural and cytoarchitectonic probabilistic maps. *Korean J Nucl Med* 2004; 38: 241-52.
- [9] Ashburner J, Friston KJ. Nonlinear spatial normalization using basis functions. *Hum Brain Mapp* 1999; 7: 254-66.
- [10] Lancaster JL, Fox PT, Downs H, *et al.* Global spatial normalization of human brain using convex hulls. *J Nucl Med* 1999; 40: 942-55.
- [11] Robbins S, Evans AC, Collins DL, Whitesides S. Tuning and comparing spatial normalization methods. *Med Image Anal* 2004; 8: 311-23.
- [12] Talairach J, Tournoux P. *Co-planar stereotaxic atlas of the human brain: 3-dimensional proportional system - an approach to cerebral imaging*. New York, Thieme Medical Publishers. 1988.
- [13] Brett M, Johnsrude IS, Owen AM. The problem of functional localization in the human brain. *Nat Rev Neurosci* 2002; 3: 243-9.
- [14] Evans AC, Collins DL, Mills SR, Brown ED, Kelly RL, Peters TM. 3D statistical neuroanatomical models from 305 MRI volumes. *Proc IEEE Nucl Science Symp Med Imaging Conf* 1993: 1813-7.
- [15] Collins DL, Neelin P, Peters TM, Evans AC. Automatic 3D intersubject registration of MR volumetric data in standardized Talairach space. *J Comput Assist Tomogr* 1994; 18: 192-205.
- [16] Friston KJ, Holmes AP, Worsley KJ, Poline J-P, Frith CD, Frackowiak RSJ. Statistical parametric maps in functional imaging: a general linear approach. *Hum Brain Mapp* 1995; 2: 189-210.
- [17] Evans AC, Collins DL, Holmes CJ. Computational approaches to quantifying human neuroanatomical variability. In: Toga AW, John C, Mazziotta JC Ed, *Brain mapping: the methods*. San Diego, Academic Press. 1996; 343-61.
- [18] Lee JS, Lee DS, Kang KW, *et al.* Development of age, gender and ethnic specific anatomical and functional standard brain templates. *Hum Brain Mapp Conf*, 2002 [Abstract].
- [19] Koo BB, Lee JM, Kim JS, *et al.* Developing a Korean standard brain atlas on the basis of statistical and probabilistic approach and visualization tool for functional image analysis. *Korean J Nucl Med* 2003; 37: 162-170.
- [20] Zilles K, Schleicher A, Palomero-Gallagher N, Amunts K. Quantitative analysis of cyto- and receptor architecture of the human brain. In Toga AW, Mazziotta JC Ed, *Brain mapping: the methods*, 2nd edition. San Diego, Academic Press. 2002; 573-602.
- [21] Amunts K, Malikovic A, Mohlberg H, Schormann T, Zilles K. Brodmann's areas 17 and 18 brought into stereotaxic space-where and how variable? *Neuroimage* 2000; 11: 66-84.
- [22] Zilles K, Palomero-Gallagher N, Grefkes C, *et al.* Architectonics of the human cerebral cortex and transmitter receptor fingerprints: reconciling functional neuroanatomy and neurochemistry. *Eur Neuropsychopharmacol* 2002; 12: 587-99.
- [23] <http://www.fz-juelich.de/ime/index.php?index=51>.
- [24] Baird AE, Austin MC, McKay WJ, Donnan GA. Sensitivity and specificity of ^{99m}Tc-HMPAO SPECT cerebral perfusion measurements during the first 48 hours for the localization of cerebral infarction. *Stroke* 1997; 28: 976-80.
- [25] Camargo EE. Brain SPECT in neurology and psychiatry. *J Nucl Med* 2001; 42: 611-23.
- [26] Lee JS, Lee DS, Kim YK, *et al.* Probabilistic map of blood flow distribution in the brain from the internal carotid artery. *Neuroimage*. In press.
- [27] Kim BG, Lee SK, Kim JY, *et al.* Interpretation of Wada memory test for lateralization of seizure focus by use of ^{99m}technetium-HMPAO SPECT. *Epilepsia* 2000; 41: 65-70.
- [28] Kim BG, Lee SK, Nam HW, Song HC, Lee DS. Evaluation of functional changes in the medial temporal region during intracarotid amobarbital procedure by use of SPECT. *Epilepsia* 1999; 40: 424-9.
- [29] Dinov ID, Mega MS, Thompson PM, *et al.* Analyzing functional brain images in a probabilistic atlas: a validation of subvolume thresholding. *J Comput Assist Tomogr* 2000; 24: 128-38.
- [30] Mega MS, Thompson PM, Cummings JL, *et al.* Sulcal variability in the Alzheimer's brain: correlations with cognition. *Neurology* 1998; 50: 145-51.
- [31] Lee DS, Lee JS, Kang KW, *et al.* Disparity of perfusion and glucose metabolism of epileptogenic zones in temporal lobe epilepsy demonstrated by SPM/SPAM analysis on ¹⁵O water PET, [¹⁸F] FDG-PET, and [^{99m}Tc]-HMPAO SPECT. *Epilepsia* 2001; 42: 1515-22.

- [32] Kim S-K, Lee DS, Lee SK, *et al.* Diagnostic performance of [¹⁸F]FDG-PET and ictal [^{99m}Tc]-HMPAO SPECT in occipital lobe epilepsy. *Epilepsia* 2001; 42: 1531-40.
- [33] Kim YK, Lee DS, Lee SK, *et al.* Differential features of metabolic abnormalities between medial and lateral temporal lobe epilepsy: Quantitative analysis of ¹⁸F-FDG PET using SPM. *J Nucl Med* 2003; 44: 1006-12.
- [34] Lee SK, Lee DS, Yeo JS, *et al.* FDG-PET images quantified by probabilistic atlas of brain and surgical prognosis of temporal lobe epilepsy. *Epilepsia* 2002; 43: 1032-8.
- [35] Swartz BE, Tomiyasu U, Delgado-Escueta AV, Mandelkern M, Khonsari A. Neuroimaging in temporal lobe epilepsy: test sensitivity and relationships to pathology and postoperative outcome. *Epilepsia* 1992; 33: 624-34.
- [36] Delbeke D, Lawrence SK, Abou-Khalil BW, Blumenkopf B, Kessler RM. Postsurgical outcome of patients with uncontrolled complex partial seizures and temporal lobe hypometabolism on ¹⁸F-FDG-positron emission tomography. *Invest Radiol* 1996; 31: 261-6.
- [37] Lee JS, Lee DS, Park KS, Chung JK, Lee MC. Changes in the heterogeneity of cerebral glucose metabolism with healthy aging: quantitative assessment by fractal analysis. *J Neuroimaging* 2004; 14: 350-6.
- [38] Muller-Gartner HW, Links JM, Prince JL, *et al.* Measurement of radiotracer concentration in brain gray matter using positron emission tomography: MRI-based correction for partial volume effects. *J Cereb Blood Flow Metab* 1992; 12: 571-83.
- [39] Rousset OG, Ma Y, Evans AC. Correction for partial volume effects in PET: principle and validation. *J Nucl Med* 1998; 39: 904-11.
- [40] Kang KW, Lee JS, Lee DS, Lee MC. Partial volume correction of simulated PET and F-18 FDG PET from 14 normal brains. In: Senda M, Kimura Y, Herscovitch P, Ed, *Brain imaging using PET*. San Diego, Academic Press. 2002; 153-7.
- [41] Lee JS, Ishii K, Kim YK, *et al.* Is the age-related decline of cerebral glucose metabolism due to the partial volume effect or Not? *J Nucl Med* 2002; 43: 66P [Abstract].
- [42] Kang E, Lee DS, Lee JS, *et al.* Developmental hemispheric asymmetry of interregional metabolic correlation of the auditory cortex in deaf subjects. *Neuroimage* 2003; 19: 777-83.
- [43] Kang E, Lee DS, Kang H, *et al.* Age-associated changes of cerebral glucose metabolic activity in both male and female deaf children: parametric analysis using objective volume of interest and voxel-based mapping. *Neuroimage* 2004; 22: 1543-53.
- [44] Bamford J, Sandercock P, Dennis M, Burn J, Warlow C. Classification and natural history of clinically identifiable subtypes of cerebral infarction. *Lancet* 1991; 337: 1521-6.
- [45] Mead GE, Shingler H, Farrell A, O'Neill PA, McCollum CN. Carotid disease in acute stroke. *Age Ageing* 1998; 27: 677-82.
- [46] Lee HY, Paeng JC, Lee DS, *et al.* Efficacy assessment of cerebral arterial bypass surgery using statistical parametric mapping and probabilistic brain atlas on basal/acetazolamide brain perfusion SPECT. *J Nucl Med* 2004; 45: 202-6.